

## Effect of electromagnetic actuations on the dynamics of a harmonically excited cantilever beam

M. Belhaq<sup>a</sup>, A. Bichri<sup>a</sup>, J. Der Hogapian<sup>b</sup>, J. Mahfoud<sup>b,\*</sup>

<sup>a</sup> *University Hassan II-Casablanca, Laboratory of Mechanics, Casablanca, Morocco*

<sup>b</sup> *Université de Lyon, CNRS, INSA-Lyon, LaMCoS UMR5259, F-69621, France*

### ARTICLE INFO

#### Article history:

Received 23 December 2009

Received in revised form

7 March 2011

Accepted 10 March 2011

Available online 21 March 2011

#### Keywords:

Electromagnetic actuator

Cantilever beam

Hysteresis

Perturbation method

Experimentation

### ABSTRACT

The influence of electromagnetic actuators (EMAs) on the frequency response of a harmonically excited cantilever beam is investigated analytically, numerically and experimentally in this paper. Specifically, the intensity of the current generating the EMAs force is varied and its effect on the dynamic behavior of the system is analyzed. Analytical treatment based on perturbation analysis is performed on a simplified equation modeling the one mode vibration of the cantilever beam. Results indicated that EMAs produce a softening behavior in the system. Further, it is shown that as the current intensity of EMAs increases, the resonance curve shifts toward smaller values of frequency and the non-linear characteristic of the system becomes softer. The analytical predictions have been verified numerically and confirmed experimentally using a test rig.

© 2011 Elsevier Ltd. All rights reserved.

### 1. Introduction

Non-linear behavior of mechanical systems can manifest itself in various forms [1,2]. For instance, in the automotive sector, the lateral vibrations of drive systems by belts may lead to a Duffing oscillator with parametric excitations [3]. Reducing this type of behavior requires an understanding of basic phenomena from analytical and experimental viewpoint. Therefore, it is of great importance to develop a strategy for reducing vibrations with large amplitudes, determine stability criteria and controlling non-linear phenomena leading to large amplitude oscillations and hysteresis in the systems. Recent analytical results have shown that the introduction of a fast harmonic excitation in pendulum-like systems can have an effect on the elimination of hysteresis [4,5]. On the other hand, active magnetic bearings (AMBs) have proved their effectiveness in many industrial applications; they have the advantage to operate without contact and can be used in applications requiring clean or corrosive environments [6]. AMBs also have the advantage of being able to act on the shaft directly or indirectly by associating them with conventional bearings. In this case AMBs act as actuators [7,8].

In the same context, electromagnetic actuators, considered as simple means of excitation [9], can be exploited positively in industrial applications where attracting forces are needed. The

systems actuated by electromagnetic forces exhibit generally complicated behavior due to the non-linearities generated by the force. For instance, non-linear dynamics and chaos control for an electromagnetic system has been considered in [10], while active electromagnetic damping of lateral vibration of a cantilever beam, which is suitable for non-linear systems, has been investigated in [11].

The objective of this paper is to study analytically, numerically and experimentally, the influence of EMAs on the frequency response of an excited cantilever beam. Specifically, the effect of varying the intensity of the current generating the EMAs force on the dynamic behavior of the system is analyzed. The aim is to assess the possibility of tuning the first resonance frequency value of the structure by using actuators with constant current.

First, in order to capture basic phenomena and to qualify the effect of electromagnetic forces on the non-linear behavior, an analytical treatment of a one degree of freedom system consisting of a non-linear oscillator subjected to a periodic excitation is performed. The analytical treatment based on a perturbation analysis leads to an approximation of the amplitude–frequency response equation allowing the analysis of the influence of EMAs on the frequency response. Then, the numerical simulations by using finite element method were performed for several configurations as close as possible to the experiments. The objective is to examine the range of variation of the important parameters in order to choose the required air gap and current intensity leading to the suitable behavior. In order to validate the analytical and numerical predictions, experiments are realized using a test rig

\* Corresponding author.

E-mail address: [jarir.mahfoud@insa-lyon.fr](mailto:jarir.mahfoud@insa-lyon.fr) (J. Mahfoud).

composed of a clamped–free beam subjected to an external forcing and submitted to EMAs forces.

**2. Equation of motion and perturbation analysis**

The one mode motion of a cantilever beam submitted to a harmonic external excitation and to symmetric EMAs is modelled as a linear mass-spring system and written in the dimensionless form as

$$z' + cz' + z = f \cos \omega \tau + F_{em} \tag{1}$$

where  $F_{em}$  is the electromagnetic actuations given by

$$F_{em} = a_0 \left( \frac{1}{(1-z)^2} - \frac{1}{(1+z)^2} \right) \tag{2}$$

with  $z = \delta_a/\lambda$ ,  $c = \alpha/m\omega_0$ ,  $\omega_0 = \sqrt{k/m}$ ,  $\omega = v/\omega_0$ ,  $f = F/\lambda m \omega_0^2$ ,  $a_0 = C_1/\lambda^3 m \omega_0^2$  and  $\tau = \omega_0 t$ . Here  $m$  is the mass,  $\omega_0$  is the natural frequency,  $\alpha$  is the damping coefficient,  $k$  is the stiffness,  $F$  and  $v$  are the amplitude and the frequency of the external forcing, respectively. The parameter  $a_0$  is proportional to the current squared (see Section 3). The other parameters  $\lambda$  and  $C_1$ , which depend on the geometrical characteristics relating the actuators to the structure, as well as the colocalized displacement  $\delta_a$  are given in Section 3. The primes in Eq. (1) represent differentiation with respect to the time  $\tau$ . In the case under consideration, the vibrations of the cantilever beam are assumed to have small amplitudes around the trivial equilibrium. As the form of the right hand side of Eq. (2) is not suitable to be analyzed directly, it is convenient to use a truncated Taylor series expansion, according to

$$\frac{1}{(1-z)^2} - \frac{1}{(1+z)^2} \simeq 4z + 8z^3 \tag{3}$$

which results in the approximate equation of motion given by

$$z' + cz' + \Omega_0^2 z - \gamma z^3 = f \cos \omega \tau \tag{4}$$

where  $\Omega_0^2 = 1 - 4a_0$  and  $\gamma = 8a_0$ . The analysis of the dynamics of Eq. (4) can be carried out by performing a perturbation technique. To approximate periodic solutions to Eq. (4) near the primary resonance, we introduce a small bookkeeping parameter  $\varepsilon$  in the non-linear component and we express the resonance condition according to

$$\Omega_0^2 = \omega^2 + \varepsilon \sigma \tag{5}$$

where  $\sigma$  is the detuning parameter from the resonance. Assuming that damping, non-linearity and forcing are small, Eq. (4) can be

scaled as follows:

$$z'' + \omega^2 z = \varepsilon (f \cos \omega \tau - cz' - \sigma z) + \varepsilon^2 \gamma z^3 \tag{6}$$

Using the multiple scales technique [2], we seek a two-scale expansion of the solution in the form

$$z(\tau) = z_0(\tau_0, \tau_1, \tau_2) + \varepsilon z_1(\tau_0, \tau_1, \tau_2) + \varepsilon^2 z_2(\tau_0, \tau_1, \tau_2) + O(\varepsilon^3) \tag{7}$$

where  $\tau_i = \varepsilon^i \tau$  define the different time scales. In terms of the variables  $\tau_i$ , the time derivatives become  $d/d\tau = D_0 + \varepsilon D_1 + \varepsilon^2 D_2 + O(\varepsilon^3)$  and  $d^2/d\tau^2 = D_0^2 + 2\varepsilon D_0 D_1 + \varepsilon^2 D_1^2 + 2\varepsilon^2 D_0 D_2 + O(\varepsilon^3)$ , where  $D_i = \partial/\partial \tau_i$  and  $D_{ij} = \partial^2/\partial \tau_i \partial \tau_j$ . Substituting (7) into (6) and equating terms of the same power of  $\varepsilon$ , we obtain the following hierarchy of problems:

$$D_0^2 z_0 + \omega^2 z_0 = 0 \tag{8}$$

$$D_0^2 z_1 + \omega^2 z_1 = -(2D_0 D_1 + cD_0 + \sigma)z_0 + f \cos \omega \tau \tag{9}$$

$$D_0^2 z_2 + \omega^2 z_2 = -(2D_0 D_1 + cD_0 + \sigma)z_1 - (2D_0 D_2 + D_1^2 + cD_1)z_0 + \gamma z_0^3 \tag{10}$$

The solution to the first order is given by

$$z_0(\tau_0, \tau_1, \tau_2) = r(\tau_1, \tau_2) \cos(\omega \tau + \theta(\tau_1, \tau_2)) \tag{11}$$

Substituting (11) into (9) and (10) and removing secular terms, we obtain the equations of amplitude and phase

$$\begin{cases} \frac{dr}{d\tau} = Ar + H_1 \sin \theta + H_2 \cos \theta \\ r \frac{d\theta}{d\tau} = Br + Cr^3 + H_1 \cos \theta - H_2 \sin \theta \end{cases} \tag{12}$$

where  $r$  and  $\theta$  are, respectively, the amplitude and the phase. Here  $A = -c/2$ ,  $H_1 = (f\sigma/8\omega^3 - f/2\omega)$ ,  $H_2 = fc/8\omega^2$ ,  $B = \sigma/2\omega - c^2/8\omega - \sigma^2/8\omega^3$  and  $C = -3\gamma/8\omega$ . Eliminating the phase  $\theta$  from (12), we obtain the following amplitude–frequency response (third order equation in  $r^2$ ) equation

$$C^2 r^6 + 2BCr^4 + (A^2 + B^2)r^2 - (H_1^2 + H_2^2) = 0 \tag{13}$$

Fig. 1 illustrates the frequency response curves as expressed by Eq. (13) for the given parameters  $c=0.05$ ,  $f=0.1$  and for different values of  $a_0$  which is directly related to the current in the EMAs. The parameters  $c$  and  $f$  are chosen as small parameters (small damping and small amplitude of the external excitation) in order to be consistent with the perturbation analysis and the experimental conditions. The solid branches indicate stable solutions, whereas the dashed ones indicate unstable ones. Note that only solutions on the solid curves can be observed in the experiment. For validation, analytical approximations are compared to numerical integration (circles) using Runge–Kutta method. It can be seen from Fig. 1 that

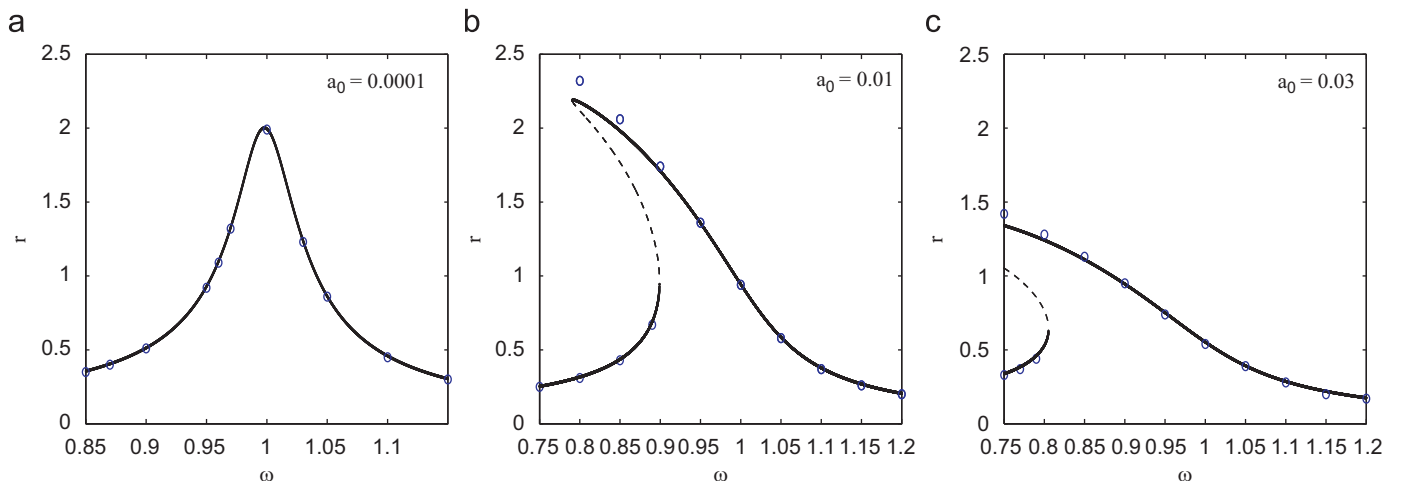


Fig. 1. Effect of  $a_0$  on the frequency–response curve for  $c=0.05$  and  $f=0.1$ . Case of two symmetric EMAs.

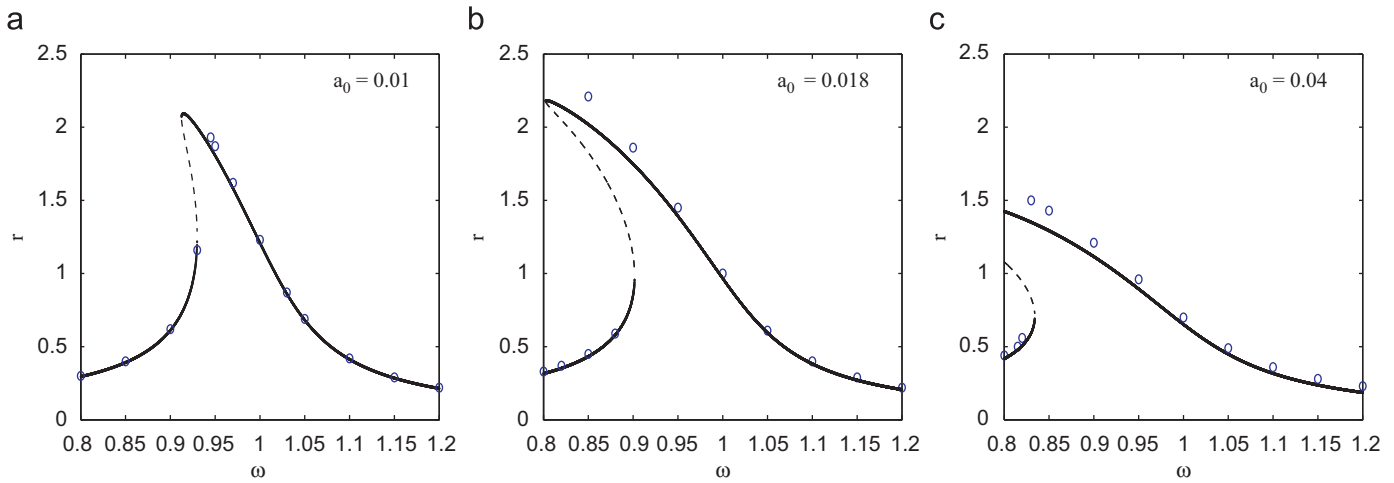


Fig. 2. Effect of  $a_0$  on the frequency–response curve for  $c=0.05$  and  $f=0.1$ . Case of asymmetric EMA.

the non-linear characteristic of the system is softening and as the intensity of the current  $a_0$  increases, the resonance curve shifts left and the softening behavior increases. For values of  $a_0$  approaching zero, the resonance curve meets the linear behavior as shown in Fig. 1a.

It is worth noticing that in the case where only one EMA is used, a similar dynamic behavior of the system can be obtained. Indeed, assume that the system is actuated by asymmetric EMA in the form

$$F_{em} = \frac{a_0}{(1-z)^2} \tag{14}$$

By using a truncated Taylor series expansion according to

$$\frac{1}{(1-z)^2} \simeq 1 + 2z + 3z^2 + 4z^3 \tag{15}$$

Eq. (1) reads

$$z'' + cz' + \Omega_0^2 z + \beta z^2 - \gamma z^3 + G = f \cos \omega \tau \tag{16}$$

where  $\Omega_0^2 = 1 - 2a_0$ ,  $\beta = -3a_0$ ,  $G = -a_0$  and  $\gamma = 4a_0$ . We express the 1:1 resonance condition by introducing a detuning parameter  $\sigma$  according to

$$\Omega_0^2 = \omega^2 + \sigma \tag{17}$$

Introducing a bookkeeping parameter  $\varepsilon$  and scaling such that Eq. (16) is written as

$$z'' + \omega^2 z = \varepsilon (f \cos \omega \tau - \sigma z - \beta z^2 - cz' - G) + \varepsilon^2 \gamma z^3 \tag{18}$$

Using the multiple scales technique, we seek a two-scale expansion of the solution in the form

$$z(\tau) = z_0(\tau_0, \tau_1, \tau_2) + \varepsilon z_1(\tau_0, \tau_1, \tau_2) + \varepsilon^2 z_2(\tau_0, \tau_1, \tau_2) + O(\varepsilon^3) \tag{19}$$

Substituting and equating terms of the same power of  $\varepsilon$ , we obtain the following hierarchy of problems:

$$D_0^2 z_0 + \omega^2 z_0 = 0 \tag{20}$$

$$D_0^2 z_1 + \omega^2 z_1 = -(2D_{01} + cD_0 + \sigma)z_0 - \beta z_0^2 - G + f \cos \omega \tau \tag{21}$$

$$D_0^2 z_2 + \omega^2 z_2 = -(2D_{01} + cD_0 + \sigma)z_1 - (2D_{02} + D_{11} + cD_1)z_0 - 2\beta z_0 z_1 + \gamma z_0^3 \tag{22}$$

The solution to the first order is given by

$$z_0(\tau_0, \tau_1, \tau_2) = r(\tau_1, \tau_2) \cos(\omega \tau + \theta(\tau_1, \tau_2)) \tag{23}$$

Substituting (23) into (21) and (22), removing secular terms, we obtain, respectively, the modulation equations of amplitude and phase (12) and the amplitude–frequency response Eq. (13) in

which the coefficients are now given by  $A = -c/2$ ,  $H_1 = (f\sigma/8\omega^3 - f/2\omega)$ ,  $H_2 = f_c/8\omega^2$ ,  $B = \sigma/2\omega - c^2/8\omega - \beta G/\omega^3 - \sigma^2/8\omega^3$  and  $C = -(3\gamma/8\omega + 5\beta^2/12\omega^3)$ . In Fig. 2 the corresponding frequency–response curves are illustrated for the same parameters as before ( $c=0.05$ ,  $f=0.1$ ) and for different values of  $a_0$ . The solid curves indicate stable solutions, whereas the dashed curves indicate unstable ones. The analytical approximations are compared to numerical integration (circles) using a Runge–Kutta method. This figure exhibits the same dynamic as in the previous case (Fig. 1), that is, the non-linear characteristic of the system is softening and as  $a_0$  increases, the resonance curve shifts toward small values of the frequency and becomes softer.

### 3. Test rig description

The experimental system illustrated in Fig. 3 is composed of a clamped–free flexible steel beam with a constant rectangular section (5 mm height and 30 mm width). The beam was clamped by fixing one end between two masses using bolted assembly. The first deflection resonance frequency is measured at 12.69 Hz, the theoretical calculated value is 12.77 Hz. The non-linearity is produced by EMAs with a constant current. Since an EMA can only produce attractive forces, two identical actuators commanded simultaneously are utilized. The actuators are placed 0.3 m from the clamped end. This position is chosen as a function of the mode shape and in order to avoid excessive displacements larger than the air gap.

Each EMA is composed of a ferromagnetic circuit and an electrical circuit. The ferromagnetic circuit is composed of two parts: an (E) shape part that receives the induction coil and an (I) shape part fixed on the beam. Both parts are composed of assemblies of insulated ferromagnetic sheets. The quality of the ferromagnetic circuit alloy is considered high enough and the nominal air gap between the stator and the beam is small enough such that the magnetic loss can be considered as negligible. The geometries of the actuators are summarized in Fig. 4.

The actuators are designed to deliver a maximum attraction force of 300 N for a maximum current of 3.0 A. The delivered attraction forces depend on the applied current that can be constant or variable. In the present study, we consider only the case of a constant current.

Based on magnetic circuit theory and assuming negligible eddy current effects and conservative flux, the relationship between the electromagnetic force  $F_{em}$ , air gap  $e$ , colocalized

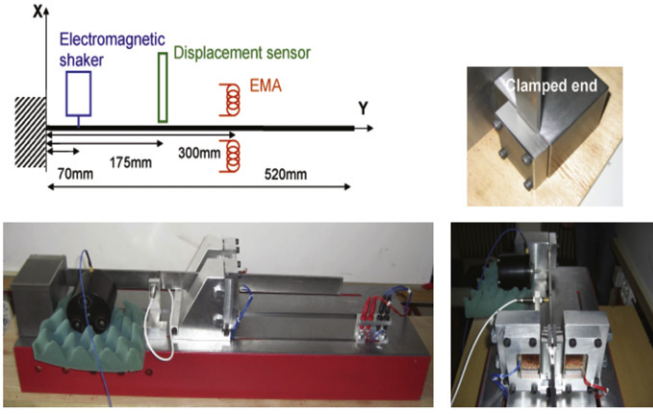


Fig. 3. Test rig.

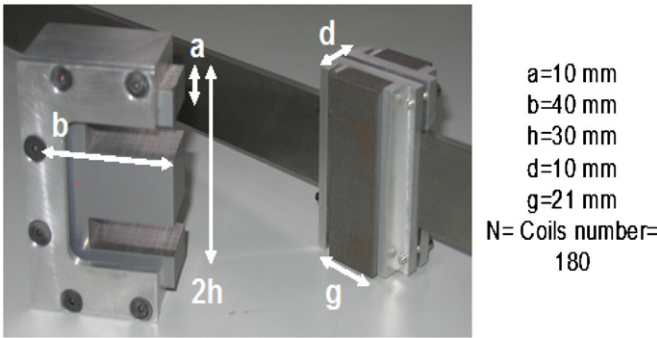


Fig. 4. EMA details.

displacement  $\delta_a$  and current  $I$  can be expressed as

$$F_{em} = \frac{N^2 \mu_0 a g I^2}{2 \left( (e \pm \delta_a(t)) + \frac{b+h+d-2a}{\mu_r} \right)^2} \quad (24)$$

The coefficients  $a$ ,  $b$ ,  $d$ ,  $g$  and  $h$  correspond to the geometrical characteristics of the actuator,  $\mu_0$  is the magnetic permeability of a vacuum ( $4\pi \times 10^{-7}$  H/m) and  $N$  is the number of coils per actuator. The coefficient  $\mu_r$  is the relative magnetic permeability (dimensionless) that is a function of the air gap and can be varied according to temperature. Its value is based on the manufacturer's specifications and is generally not known with great accuracy. In order to determine its value experimentally, the force generated by an actuator is measured for several air gaps and for different increasing and decreasing input currents [12]. The relative permeability is assumed to be constant for a low flux density and the mean value determined for the model is 740. The results obtained show that the hysteresis effect (due to electromagnetic flux) appears to be negligible and the generated forces are proportional to the current square value.

Notice that according to (24), the total electromagnetic force produced by the actuators can be expressed in the form

$$F_{em} = \frac{C_1}{\lambda^2} \left( \frac{1}{(1-z)^2} - \frac{1}{(1+z)^2} \right) \quad (25)$$

where  $C_1 = N^2 \mu_0 a g I^2 / 2$ ,  $\lambda = e + (b + h + d - 2a)\mu_r$ , and  $z = \delta_a / \lambda$ .

#### 4. Numerical investigations

This step is necessary in order to adjust and evaluate the influence of the actuator characteristics (current and air gap) on the dynamic behavior of the structure and the possibility to

introduce non-linear behavior. Numerical simulations are performed in a configuration as similar as possible to the experiment.

In order to simulate the measured responses, the structure under study is modeled by using finite elements. The chassis structure and the clamping are modeled as rigid masses, the beam is represented by 20 equal length Timoshenko beam elements with two nodes and 5 degrees of freedom, namely, three displacements and two rotations per node (along  $X$  and  $Z$  direction). The dynamic behavior of the flexible structure can be expressed in the state system presentation by

$$\begin{bmatrix} \dot{\delta} \\ \ddot{\delta} \end{bmatrix} = \dot{X} = [A]X + [B]F = \begin{bmatrix} 0 & I \\ -M^{-1}K & -M^{-1}C \end{bmatrix} \begin{bmatrix} \delta \\ \dot{\delta} \end{bmatrix} + \begin{bmatrix} 0 \\ M^{-1} \end{bmatrix} (F_{excitation} + F_{em}) \quad (26)$$

where  $[M]$  is the mass matrix,  $[K]$  is the stiffness matrix,  $[C]$  is the damping matrix,  $X$  is the state vector and  $\delta$ ,  $\dot{\delta}$ ,  $\ddot{\delta}$  are displacement, velocity and acceleration, respectively.  $[A]$  is the dynamic matrix,  $[B]$  is the command matrix and  $F_{excitation}$  is the external excitation. The effect of the EMAs,  $F_{em}$ , is considered in the second member as a restitution force.

Simulations are carried out under Matlab<sup>®</sup> and Simulink<sup>®</sup> environments. The main purpose is to analyze the dynamic behavior of the structure in the vicinity of the first mode. Calculations are performed by using modal reduction method in order to reduce simulation time. The first eight modes are considered and the damping factor utilized is 0.005 for all modes.

Fig. 5 presents the general schema of simulation. The structure response is calculated at node #7 corresponding to the displacement sensor position. The excitation force is a sinusoidal sweep of 10 Hz (5 Hz below and 5 Hz above the first resonance frequency) in 300 s. The force of 0.1 N amplitude is applied on node #3 which corresponds to the position of the electromagnetic shaker.

First, the system response is calculated for a constant current of 1 A and for several air gap values as shown in Fig. 6 (left). For relatively small air gap values (1 and 1.02 mm), the softening effects can be clearly observed, the non-dimensional value of the resonance frequency shifts from 1 to 0.4. In addition, instability zones appear for low frequencies indicating the occurrence of complex dynamics due to the non-linearity generated by the EMAs [10]. As the air gap value increases, the instability zones are attenuated and the hysteresis disappears. The curves in Fig. 6 (left) depict a softening system and confirm the shift of the frequency predicted by theory. For an important air gap value (1.4 mm), the shift of the resonance frequency is still observable and the jump phenomenon disappears.

Fig. 6 (right) illustrates the system response for an air gap of 1.2 mm and for different values of current. It can be seen in this figure that increasing the intensity of the current value amplifies

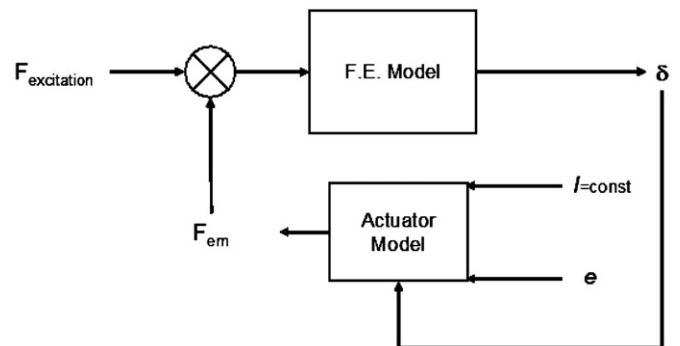


Fig. 5. Simulation schema.

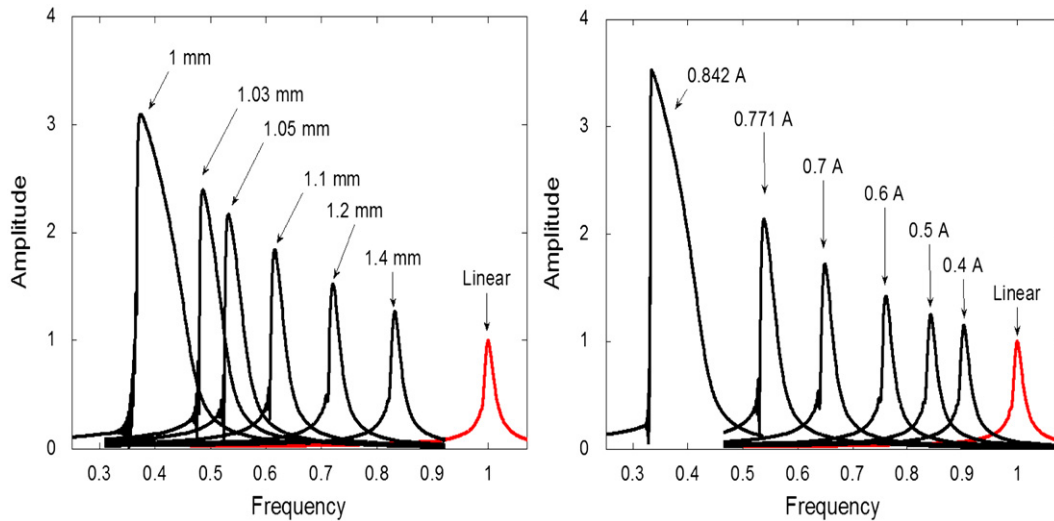


Fig. 6. System response as a function of current and gap distance variations.

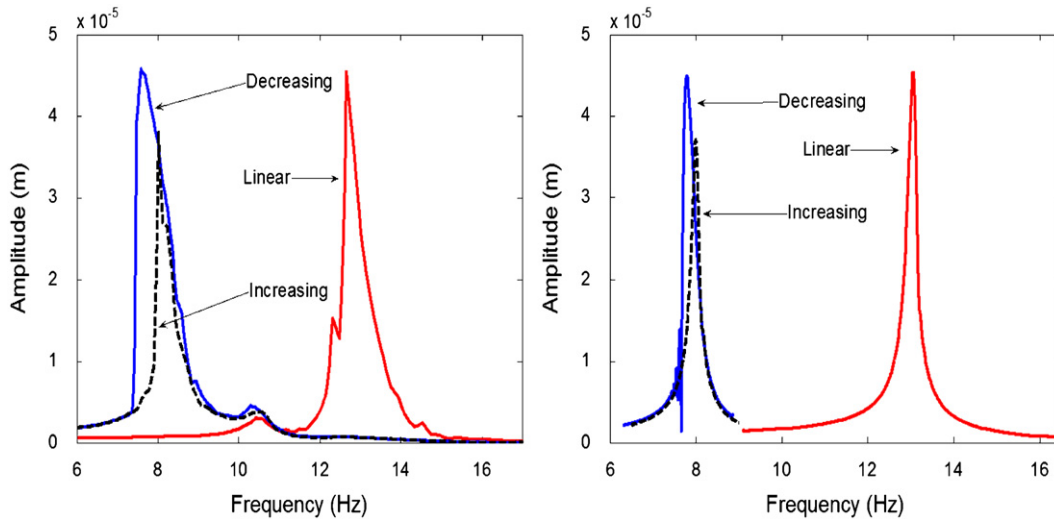


Fig. 7. Comparison between numerical (right) and experimental (left) results.

the jump phenomena and shifts the resonance frequency toward lowest values.

These results obtained by numerical simulations demonstrate the possibility of obtaining a structure whose dynamic behavior exhibits hysteresis and frequency shift by using electromagnetic forces. In addition, this non-linear behavior can be modified and controlled. The results obtained by numerical simulations are in qualitative and quantitative agreement with the analytical predictions obtained above. Next, we perform experimental testing to validate the analytical and numerical findings.

## 5. Experimental investigations

The displacements are measured by using a proximity sensor (Vibrometer TQ 102, 8 mV/ $\mu\text{m}$  sensitivity) located along the  $y$  axis. The excitation force is applied by using an electromagnetic shaker (B&K 4810, 20 N maximum force and bandwidth up to 10 KHz). The shaker is suspended by using flexible support and connected to the beam by using a pushrod near the clamped end in order to minimize the modification of the structure dynamic behavior. Given the position of the shaker, the applied force could be considered as

constant during the entire experiment. The data acquisition device used to collect experimental data is Agilent 25670A. It enables real time data acquisition and signal processing.

In Fig. 7 is illustrated the comparison between the numerical simulations (right) and the experimental investigations (left) showing a good agreement from quantitative and qualitative view points. It is worthy to point out that the analytical results are obtained for a non-dimensional single degree of freedom system that leads to qualitative results and hence comparison with experimental findings is not consistent. The chosen configuration is 1 mm air gap and 0.5 A current intensity. The amplitude of the exciting force is 1.5 N. The displacements are measured for an increasing and decreasing sinusoidal sweep from 5 to 17 Hz in 600 s. Large period of time was required in order to reach the permanent regime for each measurement. Similar conditions are applied for numerical and experimental investigations. Even though the numerical model was simple, that is no secondary phenomena noticed experimentally were taken into consideration, the general trends are still the same. It could be noticed that the first resonance frequency is shifted toward smaller values from 12.69 to 8 Hz in increasing sweep and to 7.6 Hz in decreasing sweep. Also the hysteresis phenomenon is clearly observed

via the amplitude jumps. This behavior is more accentuated in the experimental results.

This experimental observation confirms that the EMAs have a softening effect on the dynamic behavior of the structure under study for the considered frequency range.

The aim of the experiments is to assess the possibility of tuning the first resonance frequency value of the structure by using actuators with constant current. Only results for 1 mm air gap are presented. For air gap values smaller than 1 mm, it was difficult to obtain stable behavior for the considered frequency range. On the other hand, the amplitude jump phenomena were not easily identified for air gap values greater than 1 mm.

## 6. Conclusion

We have investigated analytically, numerically as well as using experimental testing, the effect of EMAs on the dynamics of a periodically excited cantilever beam. The model adopted in the analytical treatment is a linear single degree of freedom oscillator subjected to an external harmonic excitation and to EMAs forces. The multiple scales method was applied to obtain approximation of the frequency–response curve. It was shown that the force induced by the EMAs introduces a softening behavior into the system and causes the resonance curve to undergo a shift of almost 40 percent toward smaller frequencies. Further, as the intensity of the current of the EMAs force is increased, the softening characteristic of the system increases too. These results indicate that in some mechanical systems, as rotating machinery

mounted on active magnetic bearings, it is possible to tune the resonance frequency in order to avoid the critical speeds during run-up or run-down.

## References

- [1] L.N. Virgin, Introduction to Experimental Nonlinear Dynamics, Cambridge University Press, 2000.
- [2] A.H. Nayfeh, D.T. Mook, Nonlinear Oscillations, Wiley, New York, 1979.
- [3] G. Michon, L. Manin, R.G. Parker, R. Dufour, Duffing oscillator with parametric excitation: analytical and experimental investigation on a belt-pulley system, ASME Journal of Computational and Nonlinear Dynamics 3 (2008) 031001.
- [4] M. Belhaq, A. Fahsi, 2:1 and 1:1 frequency-locking in fast excited van der Pol–Mathieu–Duffing oscillator, Nonlinear Dynamics 53 (2008) 139–152.
- [5] A. Fahsi, M. Belhaq, F. Lakrad, Suppression of hysteresis in a forced van der Pol–Duffing oscillator, Communications in Nonlinear Science and Numerical Simulation 14 (2009) 2426–2433.
- [6] G. Schweitzer, H. Bleuler, A. Traxler, Active Magnetic Bearings—Basics, Properties and Applications, vdf Hochschulverlag AG, ETH, Zurich, 2003.
- [7] A. El-Shafei, A.S. Dimitri, Controlling journal bearing instability using active magnetic bearings, in: Proceedings of ASME Turbo Expo, GT2007-28059, Canada.
- [8] J. Mahfoud, Y. Skladanek, J. Der Hagopian, Active control and energy cost assessment of rotating machine, Shock and Vibration 17 (2010) 10.3233/SAV-2010-0576.
- [9] I. Gutman, Industrial Uses of Mechanical Vibrations, Business Books Limited, London, 1968.
- [10] S.C. Chang, H.P. Ling, Nonlinear dynamics and chaos control for an electro-magnetic system, Journal of Sound and Vibration 279 (2005) 327–344.
- [11] B. Gospodaric, D. Voncina, B. Bucar, Active electromagnetic damping of laterally vibrating ferromagnetic cantilever beam, Mechatronics 17 (2007) 291–298.
- [12] J. Der Hagopian, J. Mahfoud, Electromagnetic actuator design for the control of light structures, Smart Structures and Systems 6 (2010) 29–38.